OXFORD

SOT | Society of Toxicology
www.toxsci.oxfordjournals.org

TOXICOLOGICAL SCIENCES, 157(2), 2017, 410–420

doi: 10.1093/toxsci/kfx056
Advance Access Publication Date: March 24, 2017
Research article

Astrocytes Are Protective Against Chlorpyrifos Developmental Neurotoxicity in Human Pluripotent Stem Cell-Derived Astrocyte-Neuron Cocultures

Xian Wu,*,† Xiangkun Yang,‡ Anirban Majumder,§ Raymond Swetenburg,† Forrest T. Goodfellow,*,† Michael G. Bartlett,‡ and Steven L. Stice*,†,§,1

*Department of Animal and Dairy Science, Interdisciplinary Toxicology Program; †Department of Animal and Dairy Science, Regenerative Bioscience Center; ‡Department of Pharmaceutical and Biomedical Sciences, University of Georgia, Athens, Georgia 30602; and §ArunA Biomedical, Athens, Georgia 30602

The authors certify that all research involving human subjects was done under full compliance with all government policies and the Helsinki Declaration.

Disclaimer: The agency does not endorse the product.

All the experiments were carried out in accordance with the Helsinki Declaration.

[1]To whom correspondence should be addressed at *ADS Complex*, *University of Georgia*, *Athens*, *GA30602*. Fax: (706) 542-7925. E-mail: sstice@uga.edu.

ABSTRACT

Human neural progenitor cells are capable of independent, directed differentiation into astrocytes, oligodendrocytes and neurons and thus offer a potential cell source for developmental neurotoxicity (DNT) systems. Human neural progenitor-derived astrocyte-neuron cocultured at defined ratios mimic cellular heterogeneity and interaction in the central nervous system. Cytochrome P450 enzymes are expressed at a relatively high level in astrocytes and may play a critical role in the biotransformation of endogenous or exogenous compounds, including chlorpyrifos, an organophosphate insecticide that affects the central nervous system. P450 enzymes metabolize chlorpyrifos to chlorpyrifos-oxon, which is then metabolized primarily to 3, 5, 6-trichloropyridinol in addition to diethylphosphate and diethylthiophosphate. These end metabolites are less neurotoxic than chlorpyrifos and chlorpyrifos-oxon. Our objective was to identify the interactive role of astrocytes and neurons in chlorpyrifos-induced human DNT. In neuron-only cultures, chlorpyrifos inhibited neurite length, neurite number and branch points per neuron in a dose-dependent manner during a 48 h exposure, starting at 10 μM. However, in astrocyte-neuron cocultures, astrocytes protected neurons from the effects of chlorpyrifos at higher concentrations, up to and including 30 μM chlorpyrifos and endogenous astrocyte P450 enzymes effectively metabolized chlorpyrifos. The P450 inhibitor SKF525A partly negated the protective effect of astrocytes, allowing reduction in branch points with chlorpyrifos (10 μM). Thus, the scalable and defined astrocyte-neuron cocultures model that we established here has potentially identified a role for P450 enzymes in astrocytic neuroprotection against chlorpyrifos and provides a novel model for addressing DNT in a more accurate multicellular environment.

Key words: human neural progenitor; developmental neurotoxicity; astrocyte-neuron cocultures; chlorpyrifos; cytochrome P450.

The human brain consists of more than 10^{11} neurons associated with over 10^{12} glial cells. Specifically, the human cortex contains 1.4 astrocytes for every neuron (Bass *et al.*, 1971). Astrocytes contribute to homeostasis in the brain by providing neurons with energy and substrates for neurotransmission (Allen and Barres, 2009). Astrocytes are also powerful controllers of synapse formation and function plasticity in health and disease (Eroglu and Barres, 2010). Astrocytes exert protective

effects on neurons through neurotrophic factors including nerve growth factor, brain-derived neurotrophic factor, and glial cell line-derived neurotrophic factor during responses against infection, injury, cellular debris, or abnormal protein aggregates (Belanger and Magistretti, 2009; Hansebout *et al.*, 2012). In addition to neuroprotection mediated by secreted factors, astrocytes significantly contribute to the exclusion and metabolism of toxins as part of the blood-brain barrier (BBB) (Meyer *et al.*, 2001). The BBB protects the brain from fluctuations in plasma composition and from circulating agents such as neurotransmitters and xenobiotics capable of disturbing neuronal function (Abbott *et al.*, 2006). Astrocytic tripeptide glutathione (GSH) can serve as an electron donor in GSH peroxidase-catalyzed reduction of peroxides as well as act as a substrate in the detoxification of xenobiotics (Dringen *et al.*, 2015; Meyer *et al.*, 2001). Less is known about the role of astrocytes in metabolizing toxicants through other pathways.

P450 in the liver has an important role in the metabolism and detoxification of xenobiotics for subsequent elimination (Forrester *et al.*, 1992) and astrocytes express multiple forms of P450 (Kempermann *et al.*, 1994; Malaplate-Armand *et al.*, 2004). Therefore, astrocytes in a developing central nervous system (CNS) may function as a second line of defense, primarily through the BBB and second by metabolizing toxins. Thus, to assess the effect of a neurotoxic agent, it is vital to understand the innate ability of neurotoxins to cross the BBB, as well as how astrocytes metabolize toxicants that can cross the BBB.

Chlorpyrifos (CPF) is one of the most widely used insecticides in both developing and industrialized countries, including the United States (Yang *et al.*, 2011). Acute CPF exposure can lead to neurotoxicity in humans by inhibiting acetylcholinesterase-mediated breakdown of the neurotransmitter acetylcholine (Costa *et al.*, 2008). CPF can also form adducts with other proteins, impairing various molecular pathways in humans (Yang and Bartlett, 2016). The negative effects of CPF is evident over a wide neural developmental period, including early development stages affecting neural cell proliferation and differentiation, and axonogenesis (Qiao *et al.*, 2001, 2004). CPF may cross the BBB and disrupt BBB integrity and function by altering gene expression for claudin5, TRPC4 and ZO1 (Li and Ehrich, 2013). CPF alteration in BBB function is reversible upon removal of CPF (Li and Ehrich, 2013; Parran *et al.*, 2005). Metabolism of CFP by P450 in animals alters neurotoxicity. CPF-oxon (CPO) does not diminish and may enhance neurotoxicity whereas the 3, 5, 6-trichloropyridinol (TCP) metabolite is much less toxic to axonal and growth (Howard *et al.*, 2005).

Informative primary CNS cell cultures and animal studies investigated the effects of CPF and metabolites but do not address cell type specific effects, such as astrocytes. Highly enriched human astrocyte populations of human astrocytes in combination with neurons phenotypes have not been studied. In coculture studies using primary rat hippocampal astrocytes with either primary rat hippocampal neurons or rat PC12 cells, astrocytes have been shown to protect neurons against toxicity of oxidative stress (Anderl *et al.*, 2009). Recent studies suggest that astrocytes in an *in vitro* neurotoxicity test system may prove more relevant to human CNS structure and function than neuronal cells alone (Wu *et al.*, 2014). Human pluripotent stem cell (hPSC)-derived astrocytes have an integral role in the maintenance of early neuronal differentiation and neurite outgrowth (Gupta *et al.*, 2012). Human neural progenitor (hNP) cells differentiated from hPSC offer a potentially unlimited and uniform cell source for developmental neural toxicity (DNT) assays (Radio and Mundy, 2008). hNP-derived astrocytes and neurons provide an ideal platform to mimic heterotypic cellular interaction in the CNS in an *in vitro* coculture model.

Although high levels of P450 were reported in astroglial cells (Kempermann *et al.*, 1994; Malaplate-Armand *et al.*, 2004), astrocyte neuroprotective qualities are understudied and human-specific implications are unknown. We sought to more fully understand CPF effects in hPSC-derived neurons, astrocytes and astrocyte-neuron coculture systems to directly address a potential astrocyte role and mechanism in DNT protection. In this study, we show that CPF inhibited neurite outgrowth in a dose-dependent manner during 48 h exposure. However, the neurotoxic effect of CPF was rescued by the addition of astrocytes, which likely metabolized CPF. Further, a noncytotoxic low dose of a P450 inhibitor partially reversed this protective effect. Thus, for the first time, we have established a high content hPSC-derived astrocyte-neuron coculture system and identified a role for the astrocytic P450 enzyme activity in neuroprotection upon exposure to the known neurotoxicant CPF.

MATERIALS AND METHODS

Cell Maintenance

Cryopreserved hNPs, NeuroNet pure human neurons (DIV 28 neurons) and hAstroPro human astrocyte cells (ArunA Biomedical Inc., Athens, Georgia) were thawed and maintained according to manufacturer's instructions. Postthaw, live cells were counted by a trypan blue cell viability test. Cells were cultured in AB2 basal medium supplemented with ANS neural supplement (both from ArunA Biomedical Inc.), 2 mM L-glutamine (Gibco, Gaithersburg, Maryland), 50 U/ml penicillin-streptomycin (Gibco) and 10 ng/ml leukemia inhibitory factor (Millipore, Billerica, Massachusetts) on costar 96-well cell culture plate (Corning Incorporated, Corning, New York) precoated for one hour with growth factor reduced-Matrigel basement membrane matrix (R&D, Minneapolis, Minnesota) (diluted in AB2 basal medium 1:100). In the neuron-only group, DIV 28 neurons were plated at 10 000 live cells/well, while in the coculture group, DIV 28 neurons and hAstroPro were cultured at 10 000 live cells/well each.

Chemical Treatment

CPF (99.5% pure), CPO (98.5% pure), and TCP (99% pure) were all purchased from Chem Service (West Chester, Pennsylvania) and the P450 inhibitor proadifen hydrochloride (SKF-525A) from Abcam (Cambridge, Massachusetts). Test compounds were prepared as 0.15, 0.5, 1.5, 5, 15 mM stock solutions in DMSO and were then diluted to 50× in AB2/ANS, with another 10× dilution in culture to make final concentration of 0.3, 1, 3, 10, and 30 μM. SKF-525A was prepared in distilled water as stock solution: 2.5, 5, 10, 20, 40 mM with 1000× dilution in medium to make final concentrations: 2.5, 5, 10, 20, and 40 μM. Compounds were added to cell cultures 2 h after cells were seeded in 96-well culture plates and incubated for 48 h before immunocytochemical analysis.

Immunocytochemistry

Immunofluorescent staining was performed using the Eppendorf epMotion liquid handling system for automated fixing and staining. Cells were stained as described previously with minor modifications to the protocol (Gallegos-Cardenas *et al.*, 2015). Briefly, cells were fixed in 4% paraformaldehyde (Electron Microscopy Sciences, Hatfield, Pennsylvania). 100 μl of a warm (37 °C) solution of 8% paraformaldehyde were added to

culture wells containing 100 µl of medium and incubated at room temperature for 20 min (Doherty *et al.*, 2000). Fixative was then gently aspirated and cells were washed 3 times with phosphate-buffered saline (PBS) (GE Healthcare Bio-Sciences, Pittsburgh, Pennsylvania). The primary antibodies MAP2 (microtubule-associated protein 2) (1:200, EMD Millipore) and βIII-tubulin (1:1000, Abcam) were diluted in intracellular blocking solution (0.2% saponin, 2% bovine serum albumin w/v in PBS) and cells were incubated for 2 h at room temperature. Following incubation in primary antibodies, cells were washed 3 times with high salt buffer (14.6g NaCl, 1M Tris base 50 ml in 1 L distilled water) and incubated with a 1:400 dilution of DyLight 594-conjugated donkey antimouse IgG secondary antibody or DyLight 488-conjugated donkey antirabbit IgG secondary antibody (Life Technologies, Eugene, Oregon) in high salt buffer for 1 h at room temperature, protected from light. Cells were then incubated in 0.1% Hoechst 33342 (Sigma–Aldrich, St Louis, Missouri) dye in high salt buffer for 20 min, then in PBS washed 3 times with high salt buffer, and stored in PBS at 4 °C prior to image acquisition and analysis.

Image Acquisition and Analysis

A Cellomics ArrayScan VTI high-content imaging system (ThermoFisher Scientific, Waltham, Massachusetts) was used for automated image acquisition and morphometric analyses as previously described for use on hN2 cells (Harrill *et al.*, 2010). Cell body validation was quantified based on MAP2 positive expression in DIV 28 neurons. In this study, 35 fields at 20× magnification were sampled per well for cell characterization. Image analysis algorithm optimization, including nucleus validation, cell body masking and validation, and neurite tracing parameters, was performed a priori using 5 representative images from cultures with untreated DIV 28 neurons and cocultured cells. Output from high content image analysis included total cell count (cell density, % MAP2 cells per well) and measurements of neurite outgrowth (neurites per neuron, neurite length per neuron, and branch points per neuron). Briefly, nuclei were first identified by Hoechst staining (channel 1) as bright objects on a dark background (Figs. 2A and 3A). Nuclei with size and intensity values outside of the ranges determined a priori for viable cells were identified in the channel 1 image and rejected from further analyses. To determine live cells and exclude dead cells, Cellomics Neural Profiling Bioapplication was used to distinguish live cell nuclear based on average intensity and area from dead cells. The bioapplication calculated live cell nucleus Hoechst staining average intensity and area. To be considered a live cell, the nucleus had a Hoechst staining intensity below 1000 and nuclear area above 65. A cell with a nucleus with intensity score above 1000 or nuclear area below 65 was considered a dead cell and excluded for analysis as reported in Figs. 4A–C). Spatial coordinates from the channel 1 image were then superimposed on the matching MAP2 image (channel 2) to distinguish bona fide MAP2+ neurons from background noise. MAP2 cells were defined based on user-defined geometric and signal intensity-based parameters (Figs. 2B and 3B). Astrocytes were rejected through an increased threshold set based on fluorescent intensity. Positive MAP2 neurons were selected based on average fluorescent signal intensity level value (450) determined using neuron-only cultures and astrocytes were rejected based on fluorescent signal intensity threshold lower than 450 (Figs. 2B and 3B). Data were collected on a cell-by-cell basis, and values were averaged to obtain population means within each well. These well level data were treated as replicate statistical unit for analysis of neurite outgrowth.

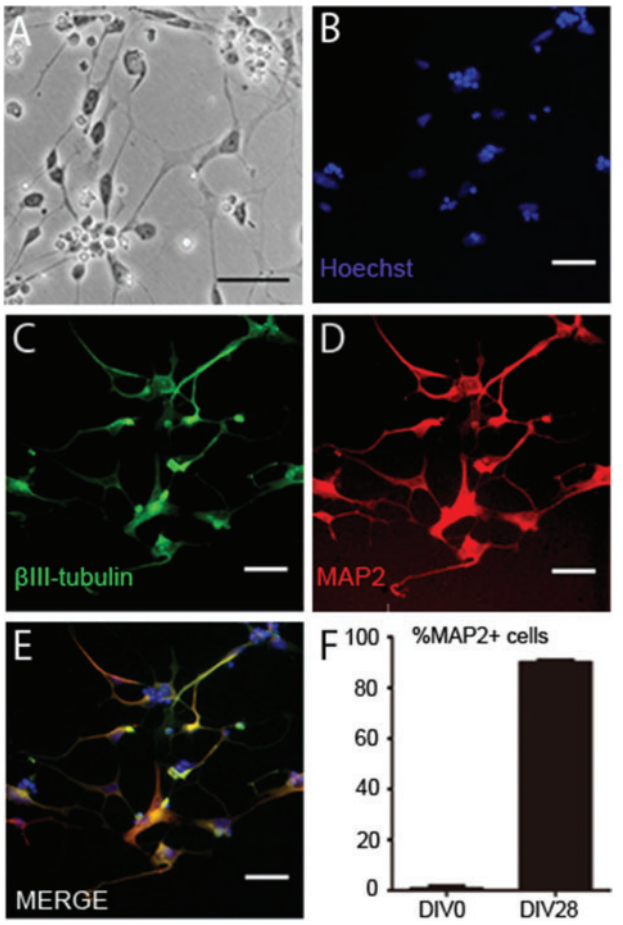

FIG. 1. DIV 28 neurons are homogenous, uniformly expressed MAP2. Human DIV 28 neuron (10 000 cells/well) was cultured for 48 h and fixed for immunofluorescent staining. A, Neuron cell phase contrast image. B, Hoechst nuclear staining. C, β-III tubulin staining of neurite outgrowth. D, MAP2 staining of neurite outgrowth. E, Hoechst, β-III tubulin, MAP2 staining merge image. F, Statistical analysis of MAP2 positive cell ratio in DIV0 hNP cells and DIV 28 neuron. Scale bars = 50 µm.

Data Acquisition and Analysis of Metabolites

Sample preparation. Each 100 µl of cell culture media was extracted with 1.7 ml isopropyl ether. The mixture was vortexed for 10 min, then centrifuged at 7500 × g, 5 °C for 10 min. 1.5 ml supernatant was transferred and evaporated at 55 °C for 10 min to complete dryness in the vacuum concentrator. The sample was reconstituted with 100 µl acetonitrile (ACN), sonicated, vortexed, and centrifuged at 7500 × g, 5 °C for 10 min 80 µl supernatant was transferred into the autosampler vial for injection.

Instrumentation. An Agilent 1100 binary pump HPLC system (Santa Clara, California) coupled with a Waters Micromass Quattro Micro triple quadrupole mass spectrometer with an ESI source (Milford, Massachusetts) was operated for LC–MS/MS analysis. Masslynx 4.0 software by Waters (Beverly, Massachusetts) was used for data processing. A Labconco CentriVap Complete Vacuum Concentrator (Kansas City, Missouri) was utilized to evaporate samples.

LC-MS/MS conditions. A Zorbax Eclipse XDB-C8 (2.1 × 150 mm, 5 µm) column coupled with a Phenomenex SecurityGuard C-8 guard column (4.0 × 2.0 mm) was used to separate the analytes. The column temperature was controlled at 32 °C. The mobile

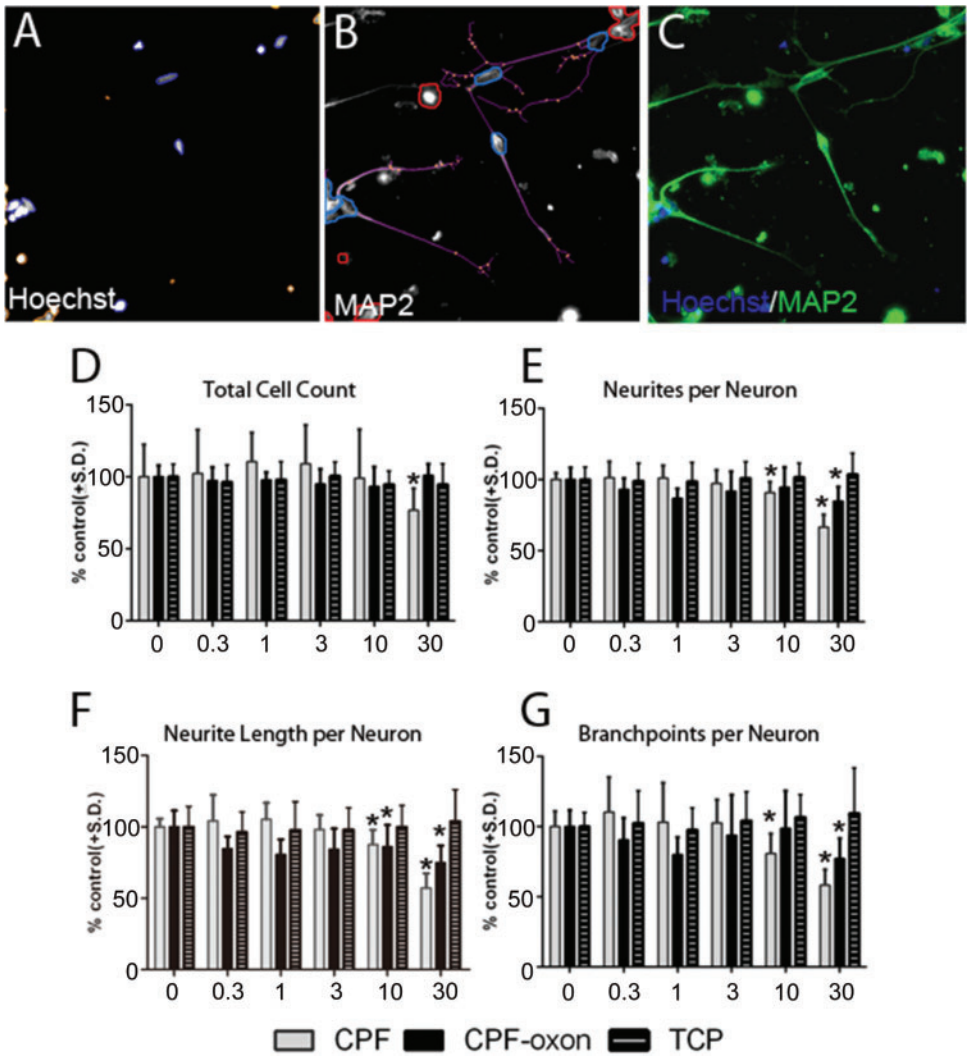

FIG. 2. CPF, CPO reduced neuron density and neurite outgrowth but TCP was nontoxic. Human DIV 28 neuron cells (10 000 cells/well) were continuously exposed to a range of doses of CPF, CPO and TCP for 48 h. A (Channel 1), Nuclei identification. Blue trace, accepted; Yellow trace, rejected. B (Channel 2), Cell body masks based on MAP2 expression; Blue trace, accepted cell; Red trace, rejected cell; Purple line, neurite; Yellow dot, branch point. Cells marked as rejected are not included calculating neurites per neuron or neurite length per neuron. Neurites emerging from accepted cell bodies are traced (purple lines) and quantified. C, Pseudo-colored images from (A) and (B) merged. D, Total neuron density (cell density) were measured as an indicator of cell viability. E–G, Average number of neurites per neuron, total neurite length per neuron and total branch points per neuron were also measured. All data are presented as % from untreated control wells. (*) indicates significant difference from control group as determined by 1-way ANOVA, $P < .05$).

phase A was 0.025% formic acid in water, mobile phase B was ACN. The injection volume was 15 µl. Analytes were separated using a gradient method, with a 0.3 ml/min flow rate, (time/minute, % mobile phase B): (0, 60), (2, 80), (2.01, 80), (5, 80), (6, 60), (10, 60). The LC system was interfaced by a 6-port divert valve to the mass spectrometer, introducing eluents to the ion source. The autosampler injection needle was washed with methanol after each injection. Samples were analyzed by the mass spectrometer in negative ion mode for TCP. Nitrogen was used as the desolvation gas at a flow rate of 500 L/h. The desolvation temperature was 500 °C and the source temperature was 120 °C. Argon was used as the collision gas and the collision cell pressure was 3.5 × 10-3 mbar. The capillary voltage was 4 kV andthe cone voltage was −22 V for TCP. A selected ion recording of 198 was applied for the quantitation of TCP. Diisopropyl ether, LC-MS grade ACN, methanol, water, and formic acid were purchased from Sigma–Aldrich. TCP was detected at a retention time of 2.35 min using a TCP standard.

Statistics

Concentration-response experiments in Figures 2 and 4 as well as P450 inhibition experiment in Figure 5 were analyzed using 1-way ANOVA with a significance threshold of $P < .05$ followed by a Tukey's test. Neuronal total cell count and neurite outgrowth in coculture was analyzed using 2-way ANOVA with a significance threshold of $P < .05$ (Figure 5 and Supplementary Figure 3). Mean values ± SD for all measurements are provided throughout the text. Statistical analyses were performed using Graphpad Prism 5.

RESULTS

MAP2 Expression Marks Neurites in a Pure Neuronal Population Derived From hNP Cells

The NeuroNet cells derived from hNP cells and cryopreserved after 28 days of differentiation (DIV 28) exhibit typical neuronal morphology within 48 h postthaw, and cultures include robust

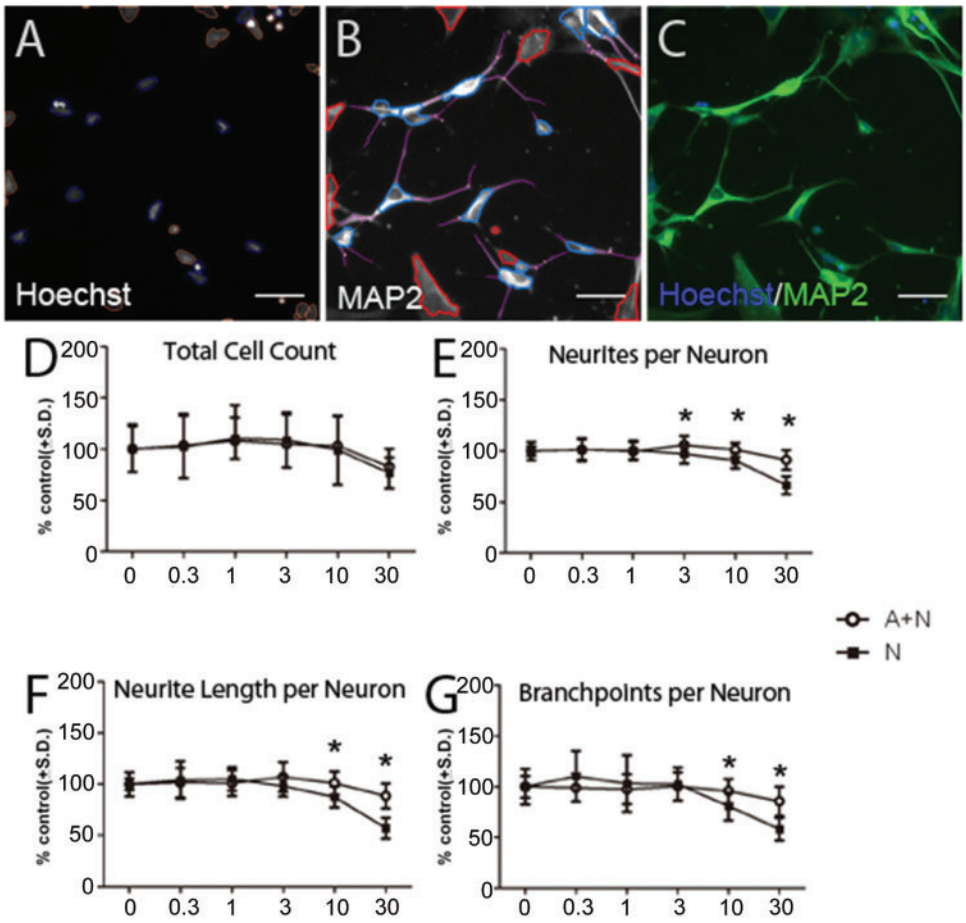

FIG. 3. CPF toxicity in DIV 28 neuron was reduced when astrocytes were cocultured with neurons. Human DIV 28 neurons (10 000 cells/well) were separately and cocultured with astrocytes (10 000 astrocytes and 10 000 neurons) for 48 h and fixed for immunofluorescent staining. MAP2 positive neuron density as well as neurite outgrowth parameters were quantified in neuron and cocultured groups. A (Channel 1), Nuclei identification. Blue trace, accepted; Yellow trace, rejected. B (Channel 2), Cell body masks based on MAP2 expression; Blue trace, accepted cell; Red trace, rejected cell; Purple line, neurite; Yellow dot, branch point. Cells marked as rejected (astrocytes and debris) are not included calculating neurites per neuron or neurite length per neuron. Neurites emerging from accepted cell bodies are traced (purple lines) and quantified. C, Pseudo colored images from (A) and (B) merged. D, Total neuron density (cell density) was counted as an indicator of cell viability. E–G, Neurite outgrowth parameters were measured. All data are presented as % from untreated control wells. (*) indicates significant difference between coculture and neuron group at the same concentration (2-way ANOVA, $P < 0.05$). Scale bars, 50 μm.

neurite outgrowth (Figure 1A). To characterize these cultures in terms of neuronal maturity, we colabeled the cells with the neuron-specific markers βIII-tubulin and MAP2 (Figs. 1C and D, respectively). Both βIII-tubulin and MAP2 were present in 96.5% of viable cells and were localized in cell bodies and neurites (Figure 1E). hNP cell cultures were negative for MAP2 expression (Figure 1F).

CPF Reduces Cell Density and Inhibits Neurite Outgrowth

To compare the inhibitory effect of CPF with its metabolites CPO and TCP on DIV 28 neurons, cells were incubated with a serial concentration of all 3 chemicals. Following continuous exposure for 48 h, cells were immunostained with MAP2 and quantified in a high content imaging system (Figs. 2A–C). CPF reduced cell density only at the highest concentration tested, 30 μM, by 23% (Figure 2D) while CPO and TCP had no effect at any of the concentrations tested (Figure 2D). CPF inhibited neurites per neuron, neurite length per neuron, and branchpoints per neuron at 10 μM (9%, 12%, 19% reductions, respectively) without reducing cell density (Figs. 2E–G). CPO, while not affecting cell density at any concentration, inhibited neurite length per neuron by 14% at 10 μM, and neurites per neuron, neurite length per neuron, and branchpoints per neuron at 30 μM by 15%, 25%, 22% (Figs. 2E–G). TCP incubation did not reduce cell density or inhibit any of the neurite outgrowth parameters (Figs. 2D–G) at the same concentrations.

Astrocytes Reduce Toxic Effect of CPF on Neurons

To investigate possible modulation of CPF neurotoxicity on DIV 28 neurons in the presence of astrocytes, 2 groups, neuron-only and astrocyte-neuron cocultures, were incubated with CPF. Cell numbers and neurite outgrowth parameters were then quantified in high content imaging system using MAP2-positive cells (Figs. 3A–C). Both total cell density and neurite outgrowth were compared between neuron-only and astrocyte-neuron cocultures groups. The presence of astrocytes did not significantly alter CPF-induced toxicity on cell density (Figure 3D). However, astrocytes rescued neurite number, neurite outgrowth and branchpoint phenotypes (Figs. 3E–G, respectively). Neurites per neuron were increased in cocultures by 10% at 10 μM and 24% at 30 μM (Figure 3E). Neurite length per neuron was increased in the cocultured group by 13% at 10 μM and 31% at

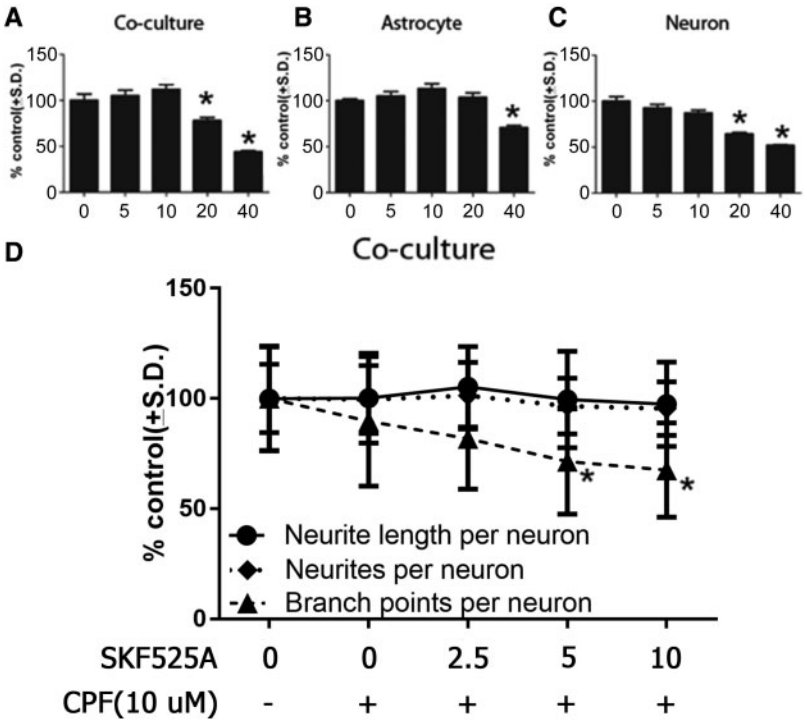

FIG. 4. SKF525A inhibited P450 activity and reversed astrocyte neuroprotective effects against CPF toxicity. Coculture cells (10 000 astrocytes and 10 000 DIV 28 neurons), astrocytes (10 000 cells/well) and DIV 28 neurons (10 000 cells/well) were seeded in 96-well plate and exposed to a range of doses of SKF525A (5, 10, 20, and 40 μM) for 48 h to determine SKF 525A noncytotoxic doses. Viable neurons and astrocytes were determined via nuclear area and intensity parameters. A, Combined viable neuron and astrocyte cells exposed to SKF525A were quantified in cocultures. B, Viable astrocyte cells exposed to SKF525A analysis. C, Viable neurons alone exposed to SKF525A, neurons were more sensitive to SKF525A than astrocytes. D, Coculture cells (10 000 astrocytes and 10 000 DIV 28 neurons) were plated for continuously exposure to CPF (10 μM) in combination with a range of noncytotoxic doses of SKF525A (2.5, 5, and 10 μM) for 48 h. Average number of neurites per neuron, total neurite length per neuron and total branch points per neuron were determined. (*) indicates significant difference from control group (1-way ANOVA, $P < .05$).

30 μM (Figure 3F). Branchpoints per neuron were increased in cocultured group by 14.99% at 10 μM and 27.34% at 30 μM (Figure 3G). Both a positive and a negative contemporary control compounds were used. Bisindolylmaleimide I (Bis-I) was the positive control for this study (Supplementary Figure 2). Bis-I interferes with cytoskeleton function in neurons and was used as a positive control in our studies since we and others have previously published on the effects of this compound in DNT human neurite assays (Harrill *et al.*, 2010; Wu *et al.*, 2016). In both neuron-only and in cocultures Bis-I at noncytotoxic doses affected neurite outgrowth parameters. The branchpoint per neuron was significantly different in neuron-only versus coculture group and neurites per neuron, neurite length per neuron, and branchpoint per neuron per field was different between neuron-only and coculture groups (Supplementary Figure 2). In addition, amoxicillin, has low neurotoxicity and none was observed at the doses used and served as the negative control (Supplementary Figure 1).

P450 Inhibitor Reduces Effects of Astrocyte on CPF Neurotoxicity in Cocultures

We next interrogated the potential role of P450 as a mediator of astrocytic neuroprotection using the P450 inhibitor SKF525A. To determine a safe dose, a series of concentrations of the SKF525A were added in the absence of CPF to the astrocyte-only, neuron-only and cocultured groups. In the cocultured group, cell density was inhibited by 20 and 40 μM SKF525A but not at lower concentrations (Figure 4A). Cell density was reduced by 29% in the astrocyte-only group at 20 μM SKF525A (Figure 4B). In the neuron-only group, cell density was decreased at 20 and 40 μM by 35% and 48% (Figure 4C). Based on these cytotoxicity results (Figs. 4A–C), 10 μM SKF525A was chosen for further studying the role of P450 in CPF metabolism since this dose was not toxic to both astrocytes and DIV 28 neurons. In the cocultured group, CPF did not inhibit neurite length and number of neurites per neuron in presence of SKF525A. However, branchpoints per neuron decreased in a dose-dependent manner in presence of SKF525A (67%–71% in 5 and 10 μM, respectively, Figure 4D). Taken together, our data indicate that astrocyte P450 activity has a role in reversing at least some DNT effects of CPF.

CPF Metabolism to TCP in Astrocyte Is Reduced by P450 Inhibitor

To test whether astrocytic P450 might impart neuroprotection by metabolizing neurotoxic CPF to the nontoxic TCP, similar to the role of P450 in the liver (Lee *et al.*, 2009), we quantified TCP by LCMS in media from neuron-only, astrocyte-only, and cocultured cell populations in the presence and absence of SKF525A (Figs. 5A–F). TCP levels in astrocytes and neurons cultured in the absence of CPF were first quantified to validate the system. Both astrocytes and neurons cell lysis have no TCP detected as shown in Supplementary Figure 3. In the neuron-only group, levels of TCP detected in media were not different in the presence and absence of SKF525A. However, TCP levels in astrocyte-only and coculture media were significantly higher in the absence of SKF525A as shown by preliminary peak area quantification (Figs. 5A–F). In the astrocyte group, TCP concentrations in media detected by LCMS quantification were 1011 ng/ml after 48 h incubation with CPF. In the astrocyte-only group with both CPF and SKF525A treatment, the TCP concentration was 67 ng/ml. In cocultures, TCP concentration was 1347 ng/ml after 48 h

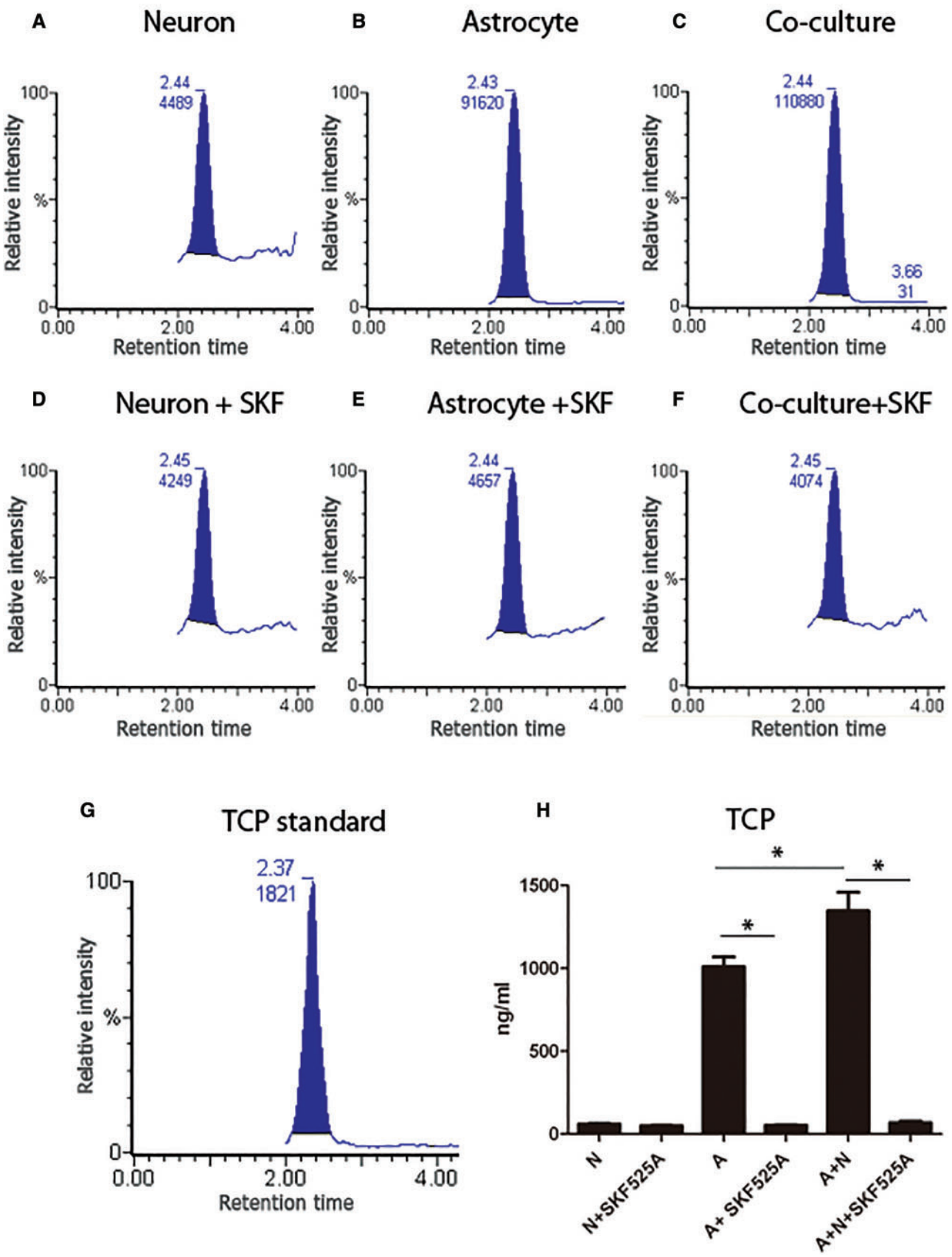

FIG. 5. CPF metabolized to TCP in presence of astrocyte. Human DIV 28 neuron (1.5×10^6 cells/well in 6-well plate), astrocytes (1.5×10^6 cells/well in 6-well plate) and coculture cells (1.5×10^6 astrocytes and 1.5×10^6 neurons in coculture in 6-well plate) were continuously exposed to CPF (10 μM) in presence or absence of SKF525A (10 μM) for 48 h. A–C, Quantification of chlorpyrifos metabolite TCP in neurons, astrocytes and coculture medium after 48 h exposure to chlorpyrifos (10 μM). D–F, Quantification of chlorpyrifos metabolite TCP in DIV 28 neuron, astrocyte and coculture medium after 48 h exposure to chlorpyrifos (10 μM) and SKF525A (10 μM). G, Quantification of TCP Standard. H, Analysis of TCP concentration in medium of neuron, astrocyte and coculture with or without SKF525A (10 μM). (1-way ANOVA, $P < 0.05$). Retention times for analytes are shown in minutes.

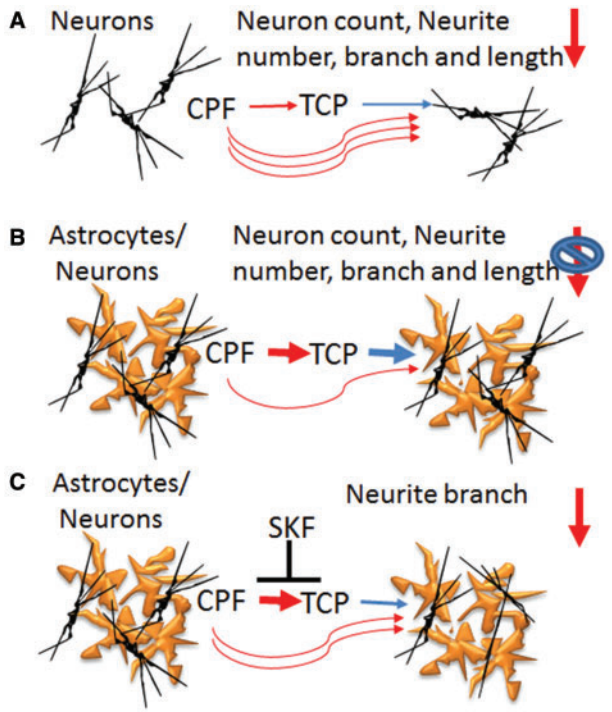

FIG. 6. Mechanistic model for an astrocyte role in reducing chlorpyrifos neurotoxicity. A, Chloypyrifos inhibited average number of neurites per neuron, total neurite length per neuron and total branch points per neuron as well as neuron density when exposed to DIV 28 neural cells. B, Astrocyte metabolized chloypyrifos to TCP and thus reduced the toxic effect of chlorpyrifos on neurite outgrowth and branching. C, Inhibition of P450 in astrocyte reduced chlorpyrifos metabolism and leaded to branching inhibition in coculture.

incubation with CPF without SKF525A. In the coculture group with both CPF and SKF525A treatment, TCP concentration decreased to 54 ng/ml. In neuron-only cultures, SKF525A caused no significant difference in TCP concentrations (61 ng/ml in the absence of SKF525A, 51 ng/ml in the presence of SKF525A (Figure 5G). TCP concentration (1347 ng/ml) in the coculture group was significantly higher than in the astrocyte group (1011 ng/ml) in absence of SKF525A (Figure 5G).

A schematic summarizes our observations and conclusions on the mechanism of action of CPF neurotoxicity on neurite outgrowth including cell density, neurite number, neurite length, and branch points per neuron (Figure 6A). In the presence of astrocytes, CPF neurotoxicity was significantly reduced on all neurite outgrowth measurement through metabolism of CPF to TCP by P450 (Figure 6B). When P450 activity in astrocyte was inhibited by SKF525A, CPF metabolism to TCP was blocked in astrocytes reducing their ability to protect neurons from CPF-induced neurotoxicity (Figure 6C).

DISCUSSION

Greater than 70 000 chemicals in commerce need regulatory testing, thus, less expensive high-throughput *in vitro* systems are needed to prioritize chemicals (Schaefer, 1994). Use of a controlled coculture of human neurons and astrocytes could provide the CNS tissue representation needed to uniformly and reproducibly predict neurotoxicities for large sets of compounds. We used highly enriched neurons and astrocytes which should reduce variability within and between screening campaigns. It also allows for defined ratios of astrocytes to neurons in cocultures, which provides a more accurate and physiological representative *in vitro* model mimicking *in vivo* neural tissue where regional differences in astrocytes to neurons ratios are documented (Herculano-Houzel, 2014; Woehrling *et al.*, 2007). Reported glia to neuron ratios varies, from 1:1 to 10:1 glia-neuron ratio, and the proportion of glial to neuronal cells depended on the human CNS regions that was examined (Herculano-Houzel 2014; Hilgetag and Barbas, 2009). Thus, it is advantageous to have a flexible system, like that reported here, where ratios could be altered to represent differing studies. Our hPSC-derived neuron-astrocyte coculture DNT system provided further insights into how astrocytes provide neuroprotective effects. Interestingly, we showed that CPF metabolism to non-toxic TCP was more efficient in astrocytes in coculture than in the astrocyte-only cultures, potentially indicating an interactive role between astrocytes and neurons in CPF metabolism. This type of information can only be observed in systems where cell types are both screened in isolation and in combination with other CNS cell types.

Although the concept of an *in vitro* cell-based DNT system is not new, the majority of reported systems either depend on primary cells sourced from animals, limiting scalability, throughput, uniformity and species representation, or on transformed cells. In contrast, nontransformed potentially unlimited lineage-restricted cell source that is easily scalable for high-throughput DNT screening has advantages (Fukushima *et al.*, 2016). Here, hNP cells differentiated for 28 days (NeuroNet) were highly enriched for cells expressing the mature neuronal marker MAP2 and Tuj-1, demonstrating purity and maturity of the neurons. Combined with a pure human astrocyte population, we achieve a controlled coculture, unlike cocultures established with primary cells that may contain contaminating cell types as well as varying astrocyte to neuron ratios among primary preparations (Kidambi *et al.*, 2008).

In regions of agriculture where CPF was used, 70% of pregnant mothers had detectable levels of CFP in their circulation. Blood levels of CPF ranged from nondetectable to 3.95 μM in pregnant women and from nondetectable to about 4.92 μM in newborns (Huen *et al.*, 2012). In patients with acute CPF poisoning, blood CPF concentration can reach 12 μM (Eyer *et al.*, 2009). These concentrations are in the range of CPF dosage in this study suggesting these were representative doses of potential CPF exposure in the CNS. Although CPF metabolism studies focus on liver microsomes and hepatocytes due to abundance of P450, it does not rule out other route of CPF exposure such as inhalation. CPF crosses the BBB (Parran *et al.*, 2005) and like other small molecules, it is plausible that a portion of inhaled CPF may also bypass circulation and pass directly into the CNS via the olfactory bulb. Also, a lack of circulating CPO in serum suggests that metabolic activation within the CNS may be responsible for CPF neurotoxicity (Khokhar and Tyndale, 2012). Recently the important contributing role of astrocytes P450-mediated metabolism in drug or neurotoxin metabolism helped decipher toxicity when plasma levels did not predict drug or toxin response (Miksys and Tyndale, 2003). Therefore, neural niche specific CPF metabolism may have a major biological effect on the local neuron population.

In previous hPSC studies, CPF inhibited neurite outgrowth at approximately 50 μM in iPSC-derived neurons which was higher than what was observed in this study and at a level higher than what was observed in the report on humans exposed to CPF (mother and newborns) (Huen *et al.*, 2012). The differences in cell line sensitivity could be due to several factors. One possible reason is that in the iPSC study, measurements were not

restricted to mature MAP2+ neurons as was done in our system, where 98.5% of the cells were mature neurons (Druwe *et al.*, 2015). Human iPSC-derived neurons cocultured with rat astrocytes were used in neuronal network function assays but human and animal cell cocultures may not accurately represent the human CNS (Harrill *et al.*, 2010; Odawara *et al.*, 2014). Apart from better representation of an interactive multicellular environment, human astrocytes differ from rodent astrocytes. Human astrocytes are larger, have more complex morphologies than rat astrocytes and a total arborization length significantly greater than that of rat astrocytes *in vitro* (Oberheim *et al.*, 2009; Zhang *et al.*, 2016). In addition, fetal human astrocytes are less sensitive in terms of glutamate responses than rat astrocytes from a developmentally comparable stage (Zhang *et al.*, 2016). Taken together, our human stem cell-based astrocyte-neuron coculture model is a significant advancement in predictive neurotoxicity.

To test our DNT system, we used CPF as a neurotoxicant. CPF is metabolized in human hepatocytes to 2 other forms, CPO and TCP, with differing neurotoxicity. We assessed the effects of each form individually on the neurons. In a dose-response experiment, the highest CPF dose tested (30 μM) was cytotoxic but similar toxicities were not observed for the other 2 forms, suggesting CPF is the most cytotoxic form for this system. Analysis of neurite outgrowth in the same cultures however showed that both CPF and CPO significantly reduced one or more endpoints, such as the number of neurites, neurite length, or branch points per neuron, suggesting both forms were specifically neurotoxic. TCP, on the other hand, did not affect any of these endpoints at doses up to 30 μM. These results are consistent with studies using a zebrafish model where axon outgrowth was significantly inhibited by CPF but not TCP (Yang *et al.*, 2011).

Comparing CPF toxicity in our human neuron-astrocyte coculture system with neuron-only cultures, we saw a decrease in total cell numbers at 30 μM CPF in both. The extent of this cytotoxic effect was not significantly different in the 2 cultures, suggesting a lack of astrocytic influence on CPF-induced cell death. However, analyses of neurite outgrowth in the same cultures showed a significant effect of astrocytes on multiple endpoints. All 3 endpoints were tested and the number of neurites, neurite length, and branch points per neuron, were significantly reduced in the neuron-only cultures, as expected, at CPF concentrations lower than 30 μM. For all 3 endpoints, astrocytes significantly reduced the negative impact of CPF, suggesting a neuroprotective effect. We also screened additional compounds (amoxicillin, retinoic acid, permethrin, testosterone, diethylstilbestrol, bisphenol A). Unlike CPF exposure, for compounds that affected neurons the astrocytes were not neural protective. No significant difference was observed between neuron-only and neuron-astrocyte cocultures (Supplementary Figure 1), suggesting that the observed astrocyte protective effect is not a general phenomenon and is compound specific.

CPF is metabolized to CPO and TCP via a P450-dependent mechanism in human hepatocytes and liver microsomes, (Lee *et al.*, 2009). Human liver cells convert CPF to CPO and then to TCP (Poet *et al.*, 2003). Since the CPF metabolite TCP did not affect neurite outgrowth or cell density when tested independently on our neurons, possible conversion of CPF to TCP in cocultures could cause the observed astrocyte neuroprotective effect. This hypothesis was further supported by the known presence of P450 enzymes in astrocytes. P450 subtype CYP2B6 is responsible for metabolism of CPF to TCP in liver cells and CYP2B6 is highly expressed in human astrocytes (Miksys *et al.*, 2003). Consistent with this, we showed here that TCP metabolite concentration significantly increased in astrocytes, both alone and in coculture after a 48 h CPF exposure, when compared with the similarly exposed neuron-only group. This observed difference suggests a role for astrocytic P450-based metabolism of CPF and the observed neurite outgrowth protective results.

To investigate the role of P450 activity in astrocytes using neurite high content imaging, we added the known P450 inhibitor SKF525A to CPF treated cocultures. SKF525A (50 μM) was previously used to inhibit P450 activity (Schuh *et al.*, 2002); however, this high concentration was cytotoxic in astrocytes and neurons with neurons affected as low as 20 μM. Based on the observed decrease branch points per neuron in the presence of CPF and SKF525A, we believe the inhibitor decreased P450 mediated astrocytic metabolism of CPF to TCP and thus reversed, in part, some astrocyte protective properties branchpoints at 10 μM SKF525A. A less cytotoxic P450 inhibitor that could be used at a higher and more effective dose may have inhibited neurite number and length. It is possible that not all astrocyte protective mechanisms are mediated through P450. In a rat primary astrocyte and neuron coculture with diazinon and diazoxon, the astrocytes protective effect was attributed to modulation of neuronal GSH content (Pizzurro *et al.*, 2014). This study used similar doses of diazinon and diazoxon (1 and 10 μM) as we used here for CPF and it is plausible that astrocytes could act via multiple neuroprotective mechanisms (P450 and GSH content). Also, Neurite branching and length are regulated by different molecules (Gallo, 2011). Doublecortin, Akt, Arp2/3 have a positive role in neurite branching but not in neurite extension (Markus *et al.*, 2002; Strasser *et al.*, 2004; Tint *et al.*, 2009). CPF decreases transcript levels of doublecortin (Wang *et al.*, 2013). Together, this implies that CPF may specifically have affected the branching through separate pathways, one being altered by SKF525A, in this astrocyte-neuron coculture system.

This study implies that hNP cell-derived astrocytes metabolized neurotoxic CPF to nontoxic TCP, as demonstrated by the P450 inhibition results. In mouse primary astrocyte cultures, the xenobiotic phenytoin was affected by astrocytic P450 active metabolism (Meyer *et al.*, 2001). However, it is important to note that humans and mice are different in P450 isoform composition, expression and catalytic activities (Nelson *et al.*, 2004). CYP1A, -2C, -2D, and -3A show appreciable interspecies differences in terms of catalytic activity and some caution should be applied when extrapolating metabolism data from animal models to humans (Martignoni *et al.*, 2006). This is the first demonstration of a human stem cell-derived astrocyte P450 activity in neuroprotection. Finding an active P450-based mechanism in hNP-derived astrocytes enables further studies using this unlimited human cell source to study xenobiotic toxification and detoxification through P450 in astrocytes *in vitro*.

Further characterization of P450 subtypes in human stem cell-derived astrocytes is required. It will be important to identify P450 activity and subtypes in hNP cell-derived astrocytes not only for CPF metabolism but also for predicting metabolism of other organophosphorus pesticides. Cultured hepatic cells have reduced P450 activities in comparison with human liver due to P450 transcriptional decreases *in vitro*. The decreased activities correlate with an alteration in the expression of key transcription factors that govern P450 transcription (Rodriguez-Antona *et al.*, 2002). Since astrocytes were derived *in vitro* from hNP cells, P450 activity could also be lower in these cells compared with astrocyte P450 activity *in vivo* (Wright and Paine, 1992).

SUPPLEMENTARY DATA

Supplementary data are available at *Toxicological Sciences* online.

ACKNOWLEDGMENTS

The authors wish to thank Dr R. Tripp's Lab for providing Cellomics ArrayScan V HCS reader high-content imaging system together with Christina Elling for comments on this manuscript.

FUNDING

This work was supported by the US Environmental Protection Agency (EPA- R835551-STAR-F1), the National Science Foundation Science and Technology Center for Emergent behaviors of integrated cellular systems (CBET 0939511) and UGA Interdisciplinary Toxicology Program.

REFERENCES

Abbott, N. J., Ronnback, L., and Hansson, E. (2006). Astrocyte-endothelial interactions at the blood-brain barrier. *Nat. Rev. Neurosci.* **7**, 41–53.

Allen, N. J., and Barres, B. A. (2009). NEUROSCIENCE Glia - More than just brain glue. *Nature* **457**, 675–677.

Anderl, J. L., Redpath, S., and Ball, A. J. (2009). A neuronal and astrocyte co-culture assay for high content analysis of neurotoxicity. *J. Vis. Exp.* **27**, 1173.

Bass, N. H., Hess, H. H., Pope, A., and Thalheimer, C. (1971). Quantitative cytoarchitectonic distribution of neurons, glia, and DNa in rat cerebral cortex. *J. Comp. Neurol.* **143**, 481–490.

Belanger, M., and Magistretti, P. J. (2009). The role of astroglia in neuroprotection. *Dialogues Clin. Neurosci.* **11**, 281–295.

Costa, L. G., Cole, T. B., Jansen, K. L., and Furlong, C. E. (2008). Paraoxonase (PON1) and organophosphate toxicity. *Paraoxnases* **6**, 209–220.

Doherty, P., Williams, G., and Williams, E. J. (2000). CAMs and axonal growth: A critical evaluation of the role of calcium and the MAPK cascade. *Mol. Cell. Neurosci.* **16**, 283–295.

Dringen, R., Brandmann, M., Hohnholt, M. C., and Blumrich, E. M. (2015). Glutathione-dependent detoxification processes in astrocytes. *Neurochem. Res.* **40**, 2570–2582.

Druwe, I., Freudenrich, T. M., Wallace, K., Shafer, T. J., and Mundy, W. R. (2015). Sensitivity of neuroprogenitor cells to chemical-induced apoptosis using a multiplexed assay suitable for high-throughput screening. *Toxicology* **333**, 14–24.

Eroglu, C., and Barres, B. A. (2010). Regulation of synaptic connectivity by glia. *Nature* **468**, 223–231.

Eyer, F., Roberts, D. M., Buckley, N. A., Eddleston, M., Thiermann, H., Worek, F., and Eyer, P. (2009). Extreme variability in the formation of chlorpyrifos oxon (CPO) in patients poisoned by chlorpyrifos (CPF). *Biochem. Pharmacol.* **78**, 531–537.

Forrester, L. M., Henderson, C. J., Glancey, M. J., Back, D. J., Park, B. K., Ball, S. E., Kitteringham, N. R., McLaren, A. W., Miles, J. S., Skett, P., *et al.* (1992). Relative expression of cytochrome P450 isoenzymes in human liver and association with the metabolism of drugs and xenobiotics. *Biochem. J.* **281 (Pt 2)**, 359–368.

Fukushima, K., Miura, Y., Sawada, K., Yamazaki, K., and Ito, M. (2016). Establishment of a human neuronal network assessment system by using a human neuron/astrocyte co-culture derived from fetal neural stem/progenitor cells. *J. Biomol. Screen.* **21**, 54–64.

Gallegos-Cardenas, A., Webb, R., Jordan, E., West, R., West, F. D., Yang, J. Y., Wang, K., and Stice, S. L. (2015). Pig induced pluripotent stem cell-derived neural rosettes developmentally mimic human pluripotent stem cell neural differentiation. *Stem Cells Dev.* **24**, 1901–1911.

Gallo, G. (2011). The cytoskeletal and signaling mechanisms of axon collateral branching. *Dev. Neurobiol.* **71**, 201–220.

Gupta, K., Patani, R., Baxter, P., Serio, A., Story, D., Tsujita, T., Hayes, J. D., Pedersen, R. A., Hardingham, G. E., and Chandran, S. (2012). Human embryonic stem cell derived astrocytes mediate non-cell-autonomous neuroprotection through endogenous and drug-induced mechanisms. *Cell Death Differ.* **19**, 779–787.

Hansebout, C. R., Su, C. X., Reddy, K., Zhang, D., Jiang, C., Rathbone, M. P., and Jiang, S. C. (2012). Enteric glia mediate neuronal outgrowth through release of neurotrophic factors. *Neural Regener. Res.* **7**, 2165–2175.

Harrill, J. A., Freudenrich, T. M., Machacek, D. W., Stice, S. L., and Mundy, W. R. (2010). Quantitative assessment of neurite outgrowth in human embryonic stem cell-derived hN2 (TM) cells using automated high-content image analysis. *Neurotoxicology* **31**, 277–290.

Herculano-Houzel, S. (2014). The glia/neuron ratio: how it varies uniformly across brain structures and species and what that means for brain physiology and evolution. *Glia* **62**, 1377–1391.

Hilgetag, C. C., and Barbas, H. (2009). Are there ten times more glia than neurons in the brain?. *Brain Struct. Funct.* **213**, 365–366.

Howard, A. S., Bucelli, R., Jett, D. A., Bruun, D., Yang, D. R., and Lein, P. J. (2005). Chlorpyrifos exerts opposing effects on axonal and dendritic growth in primary neuronal cultures. *Toxicol. Appl. Pharmacol.* **207**, 112–124.

Huen, K., Bradman, A., Harley, K., Yousefi, P., Boyd Barr, D., Eskenazi, B., and Holland, N. (2012). Organophosphate pesticide levels in blood and urine of women and newborns living in an agricultural community. *Environ. Res.* **117**, 8–16.

Kempermann, G., Knoth, R., Gebicke-Haerter, P. J., Stolz, B. J., and Volk, B. (1994). Cytochrome P450 in rat astrocytes in vivo and in vitro: intracellular localization and induction by phenytoin. *J. Neurosci. Res.* **39**, 576–588.

Khokhar, J. Y., and Tyndale, R. F. (2012). Rat brain CYP2B-enzymatic activation of chlorpyrifos to the oxon mediates cholinergic neurotoxicity. *Toxicol. Sci.* **126**, 325–335.

Kidambi, S., Lee, I., and Chan, C. (2008). Primary neuron/astrocyte co-culture on polyelectrolyte multilayer films: A template for studying astrocyte-mediated oxidative stress in neurons. *Adv. Funct. Mater.* **18**, 294–301.

Lee, S., Busby, A. L., Timchalk, C., and Poet, T. S. (2009). Effects of nicotine exposure on in vitro metabolism of chlorpyrifos in male Sprague-Dawley rats. *J. Toxicol. Environ. Health A* **72**, 74–82.

Li, W., and Ehrich, M. (2013). Transient alterations of the blood-brain barrier tight junction and receptor potential channel gene expression by chlorpyrifos. *J. Appl. Toxicol.* **33**, 1187–1191.

Malaplate-Armand, C., Leininger-Muller, B., and Batt, A. M. (2004). Astrocytic cytochromes p450: an enzyme subfamily critical for brain metabolism and neuroprotection. *Rev. Neurol. (Paris)* **160**, 651–658.

Markus, A., Zhong, J., and Snider, W. D. (2002). Raf and akt mediate distinct aspects of sensory axon growth. *Neuron* **35**, 65–76.

Martignoni, M., Groothuis, G. M. M., and de Kanter, R. (2006). Species differences between mouse, rat, dog, monkey and human CYP-mediated drug metabolism, inhibition and induction. *Exp. Opin. Drug Metab. Toxicol.* **2**, 875–894.

Meyer, R. P., Knoth, R., Schiltz, E., and Volk, B. (2001). Possible function of astrocyte cytochrome P450 in control of xenobiotic phenytoin in the brain: in vitro studies on murine astrocyte primary cultures. *Exp. Neurol.* **167**, 376–384.

Miksys, S., Lerman, C., Shields, P. G., Mash, D. C., and Tyndale, R. T. (2003). Smoking, alcoholism and genetic polymorphisms alter CYP2B6 levels in human brain. *Neuropharmacology* **45**, 122–132.

Nelson, D. R., Zeldin, D. C., Hoffman, S. M. G., Maltais, L. J., Wain, H. M., and Nebert, D. W. (2004). Comparison of cytochrome P450 (CYP) genes from the mouse and human genomes, including nomenclature recommendations for genes, pseudogenes and alternative-splice variants. *Pharmacogenetics* **14**, 1–18.

Oberheim, N. A., Takano, T., Han, X., He, W., Lin, J. H. C., Wang, F., Xu, Q., Wyatt, J. D., Pilcher, W., Ojemann, J. G., Ransom, B. R., Goldman, S. A., and Nedergaard, M. (2009). Uniquely hominid features of adult human astrocytes. *J. Neurosci.* **29**, 3276–3287.

Odawara, A., Saitoh, Y., Alhebshi, A. H., Gotoh, M., and Suzuki, I. (2014). Long-term electrophysiological activity and pharmacological response of a human induced pluripotent stem cell-derived neuron and astrocyte co-culture. *Biochem. Biophys. Res. Commun.* **443**, 1176–1181.

Parran, D. K., Magnin, G., Li, W., Jortner, B. S., and Ehrich, M. (2005). Chlorpyrifos alters functional integrity and structure of an in vitro BBB model: Co-cultures of bovine endothelial cells and neonatal rat astrocytes. *Neurotoxicology* **26**, 77–88.

Pizzurro, D. M., Dao, K., and Costa, L. G. (2014). Astrocytes protect against diazinon- and diazoxon-induced inhibition of neurite outgrowth by regulating neuronal glutathione. *Toxicology* **318**, 59–68.

Poet, T. S., Wu, H., Kousba, A. A., and Timchalk, C. (2003). In vitro rat hepatic and intestinal metabolism of the organophosphate pesticides chlorpyrifos and diazinon. *Toxicol. Sci.* **72**, 193–200.

Qiao, D., Seidler, F. J., Abreu-Villaca, Y., Tate, C. A., Cousins, M. M., and Slotkin, T. A. (2004). Chlorpyrifos exposure during neurulation: Cholinergic synaptic dysfunction and cellular alterations in brain regions at adolescence and adulthood. *Dev. Brain Res.* **148**, 43–52.

Qiao, D., Seidler, F. J., and Slotkin, T. A. (2001). Developmental neurotoxicity of chlorpyrifos modeled in vitro: Comparative effects of metabolites and other cholinesterase inhibitors on DNA synthesis in PC12 and C6 cells. *Environ. Health Perspect.* **109**, 909–913.

Radio, N. M., and Mundy, W. R. (2008). Developmental neurotoxicity testing in vitro: Models for assessing chemical effects on neurite outgrowth. *Neurotoxicology* **29**, 361–376.

Rodriguez-Antona, C., Donato, M. T., Boobis, A., Edwards, R. J., Watts, P. S., Castell, J. V., and Gomez-Lechon, M. J. (2002). Cytochrome P450 expression in human hepatocytes and hepatoma cell lines: molecular mechanisms that determine lower expression in cultured cells. *Xenobiotica* **32**, 505–520.

Schaefer, M. (1994). Children and toxic substances: confronting a major public health challenge. *Environ. Health Perspect.* **102(Suppl 2)**, 155–156.

Schuh, R. A., Lein, P. J., Beckles, R. A., and Jett, D. A. (2002). Noncholinesterase mechanisms of chlorpyrifos neurotoxicity: Altered phosphorylation of Ca2+/cAMP response element binding protein in cultured neurons. *Toxicol. Appl. Pharmacol.* **182**, 176–185.

Strasser, G. A., Rahim, N. A., VanderWaal, K. E., Gertler, F. B., and Lanier, L. M. (2004). Arp2/3 is a negative regulator of growth cone translocation. *Neuron* **43**, 81–94.

Tint, I., Jean, D., Baas, P. W., and Black, M. M. (2009). Doublecortin associates with microtubules preferentially in regions of the axon displaying actin-rich protrusive structures. *J. Neurosci.* **29**, 10995–11010.

Wang, L., Ohishi, T., Akane, H., Shiraki, A., Itahashi, M., Mitsumori, K., and Shibutani, M. (2013). Reversible effect of developmental exposure to chlorpyrifos on late-stage neurogenesis in the hippocampal dentate gyrus in mouse offspring. *Reprod. Toxicol.* **38**, 25–36.

Woehrling, E. K., Hill, E. J., and Cole-Man, M. D. (2007). Development of a neurotoxicity test-system using human post-mitotic, astrocytic and neuronal cell lines in co-culture. *Toxicology* **231**, 110–111.

Wright, M. C., and Paine, A. J. (1992). Evidence that the loss of rat-liver cytochrome-P450 invitro is not solely associated with the use of collagenase, the loss of cell-cell contacts and or the absence of an extracellular-matrix. *Biochem. Pharmacol.* **43**, 237–243.

Wu, X., Majumder, A., Webb, R., and Stice, S. L. (2016). High content imaging quantification of multiple in vitro human neurogenesis events after neurotoxin exposure. *BMC Pharmacol. Toxicol.* **17**, 62.

Wu, Y., Li, K., Zuo, H. X., Yuan, Y., Sun, Y., and Yang, X. (2014). Primary neuronal-astrocytic co-culture platform for neurotoxicity assessment of di-(2-ethylhexyl) phthalate. *J. Environ. Sci.* **26**, 1145–1153.

Yang, D., Lauridsen, H., Buels, K., Chi, L. H., La Du, J., Bruun, D. A., Olson, J. R., Tanguay, R. L., and Lein, P. J. (2011). Chlorpyrifos-oxon disrupts zebrafish axonal growth and motor behavior. *Toxicol. Sci.* **121**, 146–159.

Yang, X. K., and Bartlett, M. G. (2016). Identification of protein adduction using mass spectrometry: Protein adducts as biomarkers and predictors of toxicity mechanisms. *Rapid Commun. Mass Spectrom.* **30**, 652–664.

Zhang, Y., Sloan, S. A., Clarke, L. E., Caneda, C., Plaza, C. A., Blumenthal, P. D., Vogel, H., Steinberg, G. K., Edwards, M. S. B., Li, G., Duncan, J. A., Cheshier, S. H., Shuer, L. M., Chang, E. F., Grant, G. A., Gephart, M. G. H., and Barres, B. A. (2016). Purification and characterization of progenitor and mature human astrocytes reveals transcriptional and functional differences with mouse. *Neuron* **89**, 37–53.